Modelling of partial discharge inception and extinction voltages of sheet samples of solid insulating materials using an artificial neural network

S. Ghosh and N.K. Kishore

Abstract: This work attempts an estimation of partial discharge inception and extinction voltages (PDIV and PDEV) of sheet samples of solid dielectrics due to void inclusions of different sizes using an ANN. The effect of void dimensions and also the dielectric thickness of three common insulating materials, namely, Leatherite paper, polyethylene film and Perspex sheets on PDIVs and PDEVs are examined. Further, the effect of the permittivity of the insulating materials is also examined.

1 Introduction

Partial discharges (PDs), caused in insulation systems by local defects, such as foreign particle inclusions, voids or surface inhomogeneities, give rise to a large variety of physical phenomena. Electrical overstressing caused by these defects is, to a large degree, controlled by similar physical processes and contributes to insulation degradation and breakdown while in use. A considerable volume of data has been accumulated over the last few decades on the subject of PDs. It is suggested that the physical background knowledge on PDs can be subdivided into three fields: PD models, aging and degradation models and breakdown models [1]. In an attempt to quantify the use of PDs in evaluating the quality of any insulation system, the lowest voltage at which such events is detected, the partial discharge inception voltage (PDIV), is proposed in [2]. A review of the literature [3–6] suggests that the voltage required to produce a discharge within a dielectric depends upon the void dimensions, as well as the kind of gas in the cavity and the gas pressure. However, the discharge is independent of the nature of the dielectric and of the void location [3].

This work attempts an estimation of the PDIV and the partial-discharge extinction voltage (PDEV) of sheet samples of solid dielectrics due to void inclusions of different sizes using an artificial neural network (ANN). The necessary training data are generated in the laboratory experimentally using a CIGRE-II electrode system (sphere-plane electrode). The effect of void dimensions and dielectric thickness for the three common insulating materials, namely, Leatherite paper, polyethylene film and Perspex sheet on the PDIV and the PDEV are examined. Further, the effect of the permittivity of the insulating materials on these is also examined. Two different models are developed here. In the first case, the ANN is trained using the measured values of PDIVs and PDEVs corresponding to different PD parameters related to polyethylene film and, then, the network is tested, on completion of the training, using the test data related to Leatherite paper. Further, the ability of the network to extrapolate is also tested by considering the range of input data which are not used during the training process.

Since PDIVs and PDEVs are not related to the nature of the dielectric material concerned, in the second case the PDIVs and PDEVs are modelled using the entire set of measured data. This, apart from increasing the number of training data sets, increases the range of dielectric thickness to the void depth ratio. Moreover, the thickness of the dielectric is in some cases greater than the diameter of the void.

IEE Proceedings online no. 20020193

DOI: 10.1049/ip-smt:20020193

Paper first received 6th June 2001 and in revised form 10th January 2002

S. Ghosh is with the Electrical Engineering Department, Regional Engineering College, Rourkela, India

N.K. Kishore is with the Electrical Engineering Department, Indian Institute of Technology, Kharagpur, India

2 Experimentation

2.1 Electrode system

No standard test cell is as yet available to evaluate internal PD characteristics of solid insulating materials. A three sheet laminated specimen with a clean hole punched in the middle sheet was used by earlier researchers [3, 4] for modelling the internal PD characteristics and their effect on solid insulating materials. However, this can be used for thin specimens only [7].

Several other electrodes were also devised in Europe and the US for epoxy resins [8, 9]. Based on these, an electrode called CIGRE Method-I was devised in Japan, which is generally good for the evaluation of the internal PD characteristics and their effect on mouldable insulating materials, such as epoxy resin [9]. However, it calls for a great skill in the preparation of the test specimens. Therefore it is not recommended as a standard test cell, which naturally requires simplicity and at the same time should yield good results.

Thus, the new CIGRE method, commonly known as CIGRE Method-II, has been proposed by TGI, Japan [7]. A sectional elevation of the electrode system, along with the insulation specimen and artificial void, is shown in Fig. 1.

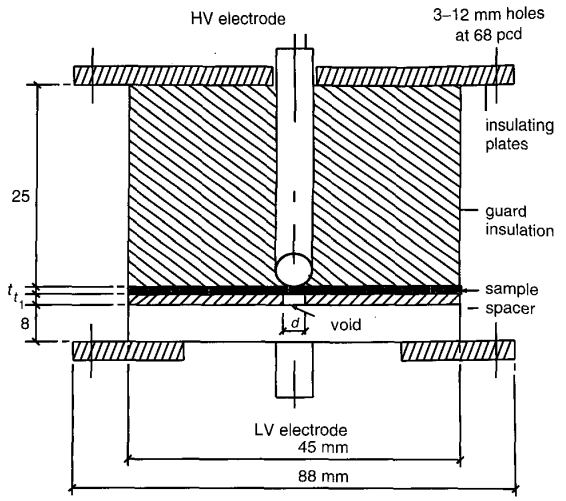

Fig. 1 *CIGRE Method II electrode system*

Considering the relative advantages of a CIGRE Method - II electrode system, over the other electrode systems used for PD testing, a test electrode is developed for this study to generate the PD data in the laboratory to be used for the modelling.

The electrode system essentially consists of a high-voltage electrode made up of a brass rod of 5.6 mm diameter, with a hemispherical end. This electrode is supported by a guard insulator made up of cast epoxy resin with a hole driven through its centre. The high-voltage electrode is push fitted centrally. The ground electrode is a plane disc of brass with a thickness of 8 mm with the necessary arrangement for connection to the ground. The pressurising arrangement, after putting in the insulation samples, is provided by two Bakelite plates, 6 mm thick, as shown in Fig. 1, with three Teflon bolts and six nuts placed at a pitch circle diameter (pcd) of 68 mm. The void is produced by a spacer made from Kapton sheets of different thicknesses.

2.2 Types of specimens

For the present investigation, the insulation specimens are prepared in the form of circular sheets, 45 mm in diameter. The thicknesses t_1 the samples considered are 0.3 mm, 0.23 mm and 0.18 mm of Leatherite paper; 0.25 mm, 0.2 mm and 0.12 mm of polyethylene film and 1 mm, 2 mm and 3 mm of Perspex sheet. Therefore the range of insulation thicknesses considered are 0.12 mm–3 mm. All the samples for a particular dimension are cut from a single sheet and care is taken so that there are no surface irregularities. The voids are created from Kapton films of 45 mm outer diameter and of different thicknesses (0.0625 mm, 0.125 mm and 0.25 mm) with a clean hole of different diameters (1 mm, 2 mm, 3 mm and 5 mm) being punched centrally, that is, the depth t and the diameter d of the voids are between 0.0625 mm–0.25 mm and 1 mm–5 mm, respectively. Suitable care is taken while punching to avoid surface irregularities.

2.3 Conditioning of the specimens

Before testing, an insulation specimen should undergo a conditioning procedure as specified by the relevant technical committee [10]. The method of cleaning and conditioning the test specimens definitely affect the test data [6].

In this work, the conditioning procedure adopted to condition the test specimen is in accordance with that laid down in the ASTM Handbook [11, 12].

2.4 Method

For the measurement of the discharge inception, the applied voltage is gradually raised until pulses corresponding to continuous discharges are first observed. This voltage is termed the inception voltage, v_i for the sample. The voltage is then gradually reduced until the discharge pulses cease. This voltage is termed as the extinction voltage, v_e for the sample. The 50 Hz AC test voltage is supplied from a 125 kV, 500 kVA series resonant dielectric test set (Hipotronics). The controlled voltage is applied to the transformer by an AC series resonant test system (Model - 7125 - 500 SR, Hipotronics). An ERA, Model-3 discharge detector (Type - 652) is used to identify the inception and extinction voltages.

Five sets of observations are made on each type of sample of a particular thickness with a particular void, for the determination of v_i and v_e and to check for the absence of external discharges. The voltages are measured by means of a voltmeter connected across the secondary of the transformer through a voltmeter resistor. To avoid supply-side disturbances, a resistor coil is connected in series with the secondary of the transformer before the power is fed to the test specimen.

3 Results and discussions

3.1 Model-1

This Section describes the PDIV, v_i and the PDEV, v_e modelling using an ANN trained with a conventional backpropagation algorithm. The network is trained with 25 sets of input/output measured data corresponding to polyethylene of thicknesses in the range of 0.12–0.25 mm. The void depth varies from 0.0625–0.25 mm and the void diameter is between 1–5 mm. On completion of training, the network is tested with nine sets of test input data (three from each dielectric thickness) corresponding to samples of Leatherite paper whose thicknesses range from 0.18–0.3 mm; with this arrangement, three sets of data, corresponding to thicknesses of 0.3 mm, are beyond the range of the training data set. Table 1 gives the complete set of measured data used for modelling of PDIVs and PDEVs.

Input-output data are normalised using (1), before the initiation of the training of the network, for better convergence and accuracy of the learning process:

$$p_i = \frac{x_i}{x_{max}} \quad i = 1, 2, \ldots, n \tag{1}$$

where x_i and x_{max} are the actual data and the maximum value of the input (or output) patterns, respectively, and n is the number of input-output pairs. The sigmoidal function is used as the activation function for all the neurons, except for those in the input layer.

To search the optimal setting of the weights, using a conventional backpropagation algorithm, the following key parameters are addressed: the ANN parameters, the number of hidden layers and hidden neurons and the evaluation criterion. Further, both on-line and batch training procedures are adopted here, and their relative effectiveness is verified.

Choice of ANN Parameters: To decide upon the optimum value of the ANN parameters, a value of the learning rate, $\eta = 0.25$ and the momentum constant, $\alpha = 0.9$, are chosen to begin with and then varied. In the range $\eta = 0.1$–0.5, the mean sum squared error for the test data, E_{ts} does not follow a typical pattern. However, a minimum value of E_{ts} of 0.0012 is obtained with $\eta = 0.25$ for number of hidden neurons = 7 and number of hidden layers = 1 after 3000 iterations.

Table 1: Measured values of PDIV and PDEV corresponding to different PD parameters and insulating materials, after correcting for atmospheric conditions

PD parameters			Inception voltage (rms)	Extinction voltage (rms)	Material
t, mm	t_1, mm	d, mm	kV	kV	
0.25	0.25	1.0	1.61	1.49	
		2.0	1.37	1.32	
		5.0	1.15	1.04[2]	
	0.125	1.0	1.27	1.06	
		2.0	1.11	1.05	
		5.0	0.84	0.79	
	0.0625	1.0	1.14	0.95	
		2.0	1.0	0.89	polyethylene
0.2	0.25	1.0	1.43	1.26	
		2.0	1.26	1.13	
		5.0	1.0	0.85	
	0.125	1.0	1.16	1.06	
		2.0	1.01	0.84	
		5.0	0.83	0.73	
	0.0625	1.0	1.08	0.91	
		2.0	1.0	0.85[2]	
0.12	0.25	1.0	1.26	1.12	
		2.0	1.16	1.06	
		5.0	0.92	0.77	
	0.125	1.0	1.18	1.07[2]	
		2.0	0.92	0.75	
		3.0	0.80	0.60	
		5.0	0.72	0.55	
	0.0625	1.0	0.70	0.55	
		2.0	0.60	0.50	
0.30	0.25	1.0	2.03	1.85	
		2.0	1.65	1.49[1,2]	
		5.0	1.36	1.14	
	0.125	1.0	1.89	1.68	
		2.0	1.51	1.32	
		3.0	1.39	1.15	
		5.0	1.09	0.98[1]	
	0.0625	1.0	1.60	1.35	
		2.0	1.20	1.09[1]	Leatherite paper
0.23	0.25	1.0	1.52	1.40[1]	
		2.0	1.40	1.30	
		5.0	1.24	1.06	
	0.125	1.0	1.36	1.14	
		2.0	1.27	1.1	
		3.0	1.08	0.95[1]	
		5.0	1.02	0.9[2]	
	0.0625	1.0	1.15	1.0	
		2.0	0.96	0.82[1]	
0.18	0.25	1.0	1.48	1.23	
		2.0	1.29	1.19	
		5.0	1.03	0.90[1]	
	0.125	1.0	1.28	1.10	
		2.0	1.05	0.92[1]	
		3.0	1.01	0.92	
		5.0	0.89	0.78	
	0.0625	1.0	1.08	0.88[1,2]	
		2.0	0.93	0.75	
1.0	0.25	1.0	3.59	3.43	
		2.0	3.30	3.19	
		5.0	2.67	2.49	
	0.125	1.0	3.04	2.83	
		2.0	2.77	2.52	Perspex
		3.0	2.56	2.38[2]	
		5.0	2.15	1.90	
	0.0625	1.0	2.61	2.38	
		2.0	2.41	2.23	
2.0	0.25	1.0	5.28	5.07	
		2.0	4.75	4.49	
		5.0	4.62	4.24	
	0.125	1.0	4.31	4.08	
		2.0	3.84	3.61	
		5.0	3.15	2.90	
	0.0625	1.0	3.40	3.1[1]	
		2.0	3.00	2.80	
3.00	0.25	1.0	6.17	5.69	
		2.0	5.70	5.40[2]	
		5.0	5.37	5.04	
	0.125	1.0	5.22	5.19	
		2.0	4.79	4.44	
		5.0	4.30	4.10	
	0.0625	1.0	4.34	4.01	

[1]Test data set used in Model I and [2]Test data set used in Model II

The values of E_{ts} for the variation of α between 0.75 and 0.95 show that the value of E_{ts} increases whenever there is a change (positive or negative) in α from 0.9. Thus the best combination of ANN parameters is seen with values of $\eta = 0.25$ and $\alpha = 0.9$. For example, when $\alpha = 0.95$, an E_{ts} value of 0.0048 is obtained as compared to 0.0012 when $\alpha = 0.9$. In the other direction the E_{ts} rises to a value of 0.0417 when $\alpha = 0.75$.

Choice of number of hidden neurons and hidden layers: The ANN structure is designed with one hidden layer and the number of hidden neurons are varied from 3–10 as before. The variation of the mean sum squared error of the testing data is observed in each case for different ANN parameters and numbers of iterations. Thus, several structures are considered with different numbers of hidden neurons to determine the best configuration.

The ANN structure with one hidden layer designed with three neurons, yields an E_{ts} of 0.0048 after 3000 iterations (with $\eta = 0.25$ and $\alpha = 0.9$). With an increase in the number of neurons, the E_{ts} decreases to a minimum value of 0.0012 when the number of hidden neurons are seven and then increases to a value of 0.003 when the number of

hidden units are 10. Therefore the best result is obtained with a network of seven hidden neurons.

When the network is designed with two hidden layers and the number of hidden neurons is varied for all the combinations in the range of 3–7 for two layers, a minimum value of $E_{ts} = 0.0022$ is obtained, corresponding to three neurons in both the layers.

Thus, a network with a single hidden layer performs well in this proposed estimation work as compared to a network with two hidden layers. A minimum E_{ts} of 0.0012 is obtained with a single hidden layer and seven neurons as compared to an error of 0.0022 for a double hidden layer network with three neurons in each layer; which is approximately twice that of the single hidden layer.

The best combination is thus seen with $\eta = 0.25$ and $\alpha = 0.9$ with a single layered network consisting of seven neurons and what follows next is based on a single hidden layer only.

Evaluation criterion: Fig. 2 shows the error distributions of the network in the proposed estimation work as a function of the number of iterations. As expected, the E_{tr} is constantly decreasing as training progresses. This is common in any mapping network. However, the odd thing is that the E_{ts} decreases for a while, but then begins to increase again. Therefore the training should be terminated at the minimum value of the E_{ts}, that is after 3000 iterations in the work presented here to avoid overtraining of the network. The number of iterations at which the training is terminated depends on the solution methodology, that is, estimation procedure, rather than the electrical properties involved.

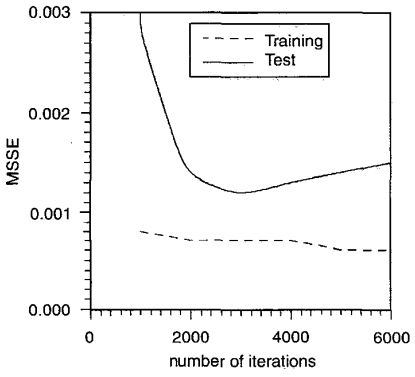

Fig. 2 *Variation of mean sum squared error as a function of iterations for the training and test data ($\eta = 0.25$, $\alpha = 0.9$, number of hidden neurons = 7 and number of hidden layers = 1)*

3.1.1 Comparison of on-line and batch learning:

Fig. 3 shows the mean squared error distributions of the test data as a function of the number of iterations for on-line and batch training procedures of the network. From the Figure, it is clear that the on-line procedure is more effective for the proposed estimation work.

From the above discussions, it is obvious that an ANN with a single hidden layer having seven hidden neurons with on-line learning gives the best result with $\eta = 0.25$ and $\alpha = 0.9$ after 3000 iterations.

Finally, the inception voltages, $v_i = f(t, t_1, d)$ and $v_e = f(t, t_1, d)$ for the test data are calculated simply by passing the input data in the forward path of the network and using the updated weights of the network. When the range of the

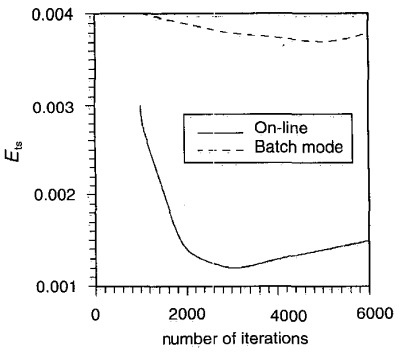

Fig. 3 *Variation of mean sum squared error as a function of iterations for on-line and batch learning procedures ($\eta = 0.25$, $\alpha = 0.9$, number of hidden neurons = 7 and number of hidden layers = 1)*

test data is within the range of the training data, an MAE of 3% is obtained. When the data corresponding to a dielectric thickness of 0.3 mm is included within the test set, the MAE increases to 3.38%. This clearly indicates the adaptibility of the network to data not included in the training set. However, the network fails to converge for the test data set corresponding to the data related to Perspex with thicknesses between 1–3 mm which are used here. This, perhaps, indicates the limitation of the network to extrapolate much beyond the certain range of the training data. To establish the capability of the proposed ANN beyond the thicknesses considered in this paper requires further experimentation, which is currently being undertaken. The programme, developed in a UNIX environment on a mainframe computer (Model: Cyber 840, 4GB HDD, 132 MHz), takes 4.7 s to complete the calculation.

3.1.2 Comparison of the estimated output with the measured values of PDIV and PDEV:

The results of the proposed estimation work are compared with the measured values and are presented in Table 2. As may be seen from this Table, an ANN can estimate the PDIV and the PDEV very well once it is trained properly and MAEs of 3.15% and 4.61% are obtained for the PDIV and then PDEV, respectively. A comparison of the measured and estimated data clearly shows that the effect of the nature of the dielectric on the PDIV and the PDEV is very

Table 2: Comparison of estimated and measured values of PDIV and PDEV ($\eta = 0.25$, $\alpha = 0.9$, number of hidden neurons = 7, number of hidden layers = 1 and number of iterations = 3000)

PDIV			PDEV		
measured kV	estimated kV	MAE %	measured kV	estimated kV	MAE %
1.52	1.5286		1.40	1.4006	
1.08	1.0215		0.95	0.8906	
0.96	1.0084		0.82	0.8647	
1.03	1.0021		0.90	0.8803	
1.05	1.0568	3.15	0.92	0.8986	4.61
1.08	1.0993		0.92	0.9527	
1.65	1.579		1.49	1.4646	
1.09	0.9873		0.98	0.9258	
1.20	1.1286		1.09	1.0147	

little. Thus, the object of the next Section is to model the PDIV and the PDEV using a combination of the measured data from the three insulation materials.

3.2 Model-II

In this Section PDIV, v_i, and PDEV, v_e, modelling is attempted using an ANN trained with an adaptive back-propagation algorithm. The network is trained with 67 sets of input/output measured data corresponding to the three common insulating materials considered in this work, polyethylene film, Leatherite Paper and Perspex sheet of thickness, t, in the range of 0.12–3 mm. The depth of the void, t_1, varies from 0.0625–0.25 mm and the void diameter, d, ranges between 1–5 mm. Thus, the ratio of the insulation thickness and void depth considered are between 0.48 (minimum) and 48 (maximum). The ratio of the insulation thickness and the void diameter considered are between 0.024 (minimum) and 3 (maximum). These ratios give an idea of the physical size of the void embedded in the dielectric concerned. Further, the above ranges are more than those reported in the literature; for example, in Mason's model [4] these ratios are $t/t_1 = 1.7$ (minimum) and 12.5 (maximum), and $t/d = 0.5$ (minimum) and 2 (maximum). On completion of the training, the network is tested with nine sets of test input data (three for each dielectic). Table 1 gives the complete set of measured data used for the modelling of the PDIV and the PDEV.

The network considered and methodology adopted here for the estimation of the PDIV and the PDEV are essentially the same as in Model-I with a single hidden layer. The backpropagation algorithm applicable to the on-line and batch learning process is used to obtain the optimal setting of the weights.

To decide upon the optimum value of the ANN parameters, values of $\eta = 0.25$ and $\alpha = 0.9$ are chosen to begin with and then varied. While varying η, it is observed that the network converges only in the range of $\eta = 0.2$ and below. Thus, η is varied between 0.05–0.2.

On the other hand, a variation of α shows no improvement below $\alpha = 0.9$ and it fails to converge above 0.9.

Finally, a best combination of the network parameters is obtained with $\eta = 0.1$ and $\alpha = 0.9$ with a single layered network consisting of 10 neurons, and a minimum value of E_{ts} is obtained as 0.0034 after 3000 iterations.

To determine the optimum number of hidden neurons, the ANN structure is designed with one hidden layer and the number of hidden neurons are varied from 3–12. Variations of E_{ts} are observed in each case for different ANN parameters and number of iterations. Thus, several structures are considered with a different number of hidden neurons to determine the best configuration.

The ANN structure designed with three and four neurons failed to converge, and the network designed with five neurons yields an E_{ts} of 0.0055 after 3000 iterations (with $\eta = 0.1$ and $\alpha = 0.9$). With an increase in the number of neurons, the E_{ts} decreases to a minimum value of 0.0034 when the number of hidden neurons are 10 and then increases to a value of 0.0045 when the number of hidden units are 12.

Fig. 4 shows the error distributions of the network in the proposed estimation work as a function of the number of iterations. As shown in the Fig. 4, the minimum test error is obtained at 3000 iterations.

From the above discussions, it is clear that an ANN with a single hidden layer having 10 hidden neurons with on-line learning gives the best result with $\eta = 0.1$ and $\alpha = 0.9$ after 3000 iterations.

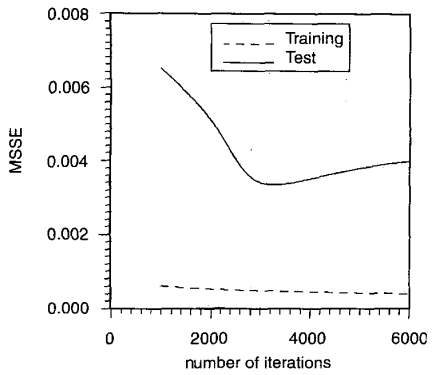

Fig. 4 *Variation of mean sum squared error as a function of iterations for the training and test data ($\eta = 0.1$, $\alpha = 0.9$, number of hidden neurons = 10 and number of hidden layers = 1)*

Finally, the inception voltages, $v_i = f(t, t_1, d)$ and extinction voltages, $v_e = f(t, t_1, d)$ for the test data are calculated simply by passing the input data in the forward path of the network and using updated network weights. The programme, developed in the UNIX environment takes 16.3 s to converge.

3.2.1 Comparison of the estimated output with the measured values of PDIV and PDEV:

The results of the proposed estimation work are compared with the measured values and are represented in Table 3. As may be seen, MAEs of 3.72% and 2.65% are obtained for the PDIV and the PDEV, respectively, for the complete set of test data. Thus, it reveals that the ANN can reliably be used for the estimation of PDIV and the PDEV with an MAE as low as 3%.

Table 3: Comparison of estimated and measured values of PDIV and PDEV ($\eta = 0.1$, $\alpha = 0.9$, number of hidden neurons = 10, number of hidden layers = 1 and number of iterations = 3000)

PDIV			PDEV		
measured	estimated	MAE	measured	estimated	MAE
kV	kV	%	kV	KV	%
1.15	1.1609		1.04	1.0193	
1.00	0.9555		0.85	0.8068	
1.18	1.1138		1.07	0.9649	
1.65	1.64		1.49	1.4863	
0.96	0.9144	3.72	0.85	0.7698	2.65
1.08	1.0397		0.88	0.8867	
2.56	2.6006		2.38	2.3809	
3.28	3.3977		3.10	3.1602	
5.75	5.8363		5.40	5.4666	

3.3 Effect of materials

To see the effect of insulating materials on the PDIV and the PDEV, the ANN is further tested for the entire range of data with the inclusion of permittivity also as an input parameter. Therefore the ANN consists of four input nodes and two output nodes.

The relative permittivities of the samples used are measured using a frequency response analyser (Model 1255HF, Solarton, Schlumberger) and are presented in Table 4.

Table 4: Relative permittivities of the insulation samples used

Insulation sample	Permittivity	
	100 Hz	1 kHz
Leatherite paper	3.36	3.1
Polyethylene	2.45	2.35
Perspex	5.73	5.26

The network is trained adaptively with an on-line learning approach for the same network parameter as in Model-II. Incidentally, for the same network parameter, a minimum value of E_{ts} of 0.0073 is obtained.

On comparision of the two estimated results, considering permittivity in one case and without permittivity in the other, it is found that the MAE is increased to 9.51% and 3.01% as compared to 3.72% and 2.65%, respectively, for the PDIV and the PDEV. Therefore changes of 5.79% and 0.36% are observed for the PDIV and the PDEV, respectively. The estimated and measured values of the PDIV and the PDEV are presented in Table 5.

Table 5: Comparison of estimated and measured values of PDIV and PDEV ($\eta = 0.1$, $\alpha = 0.9$, number of hidden neurons = 10, number of hidden layers = 1 and number of iterations = 3000)

PDIV			PDEV		
measured kV	estimated kV	MAE %	rneasured kV	estimated kV	MAE %
1.15	1.073		1.04	0.9331	
1.00	0.8717		0.85	0.722	
1.18	1.0786		1.07	0.9292	
1.65	1.546		1.49	1.3951	
0.96	0.9215	9.51	0.85	0.7968	3.01
1.08	1.1327		0.88	0.9659	
2.56	2.5654		2.38	2.3479	
3.28	3.4149		3.10	3.2018	
5.75	5.7999		5.40	5.4312	

4 Conclusions

The combination of the ANN parameters giving the best result in each model are identified. Comparison of modelled and experimental results indicates that an ANN can be used reliably within and, to some extent, beyond the training range for the estimation of PD quantities as a function of PD parameters. A comparative analysis of the modelled results with the results obtained from the empirical relations given by earlier researchers demonstrates the effectiveness of an ANN in modelling a system with an unknown nonlinear relationship. In a practical environment, measurement uncertainties of the order of $\pm 10\%$ are often acceptable. Thus, it may be said that the estimation of PDIV and PDEV using an ANN architecture in this work does not depend on permittivity. This also validates the observation of Hall and Russek [3].

5 Acknowledgments

The authors are grateful to Fort Glosters Limited, Bauria, Howrah for carrying out the experimental work.

6 References

1 NIEMEYER, L.: 'A generalized approach to partial discharge modelling', *IEEE Trans. Dielectr. Electr. Insul.*, 1995, **2**, (4), pp. 510–527
2 FORSTER, E.O.: 'Partial discharges and streamers in liquid dielectrics - the significance of the inception voltage', *IEEE Trans. Electr. Insul.*, 1993, **28**, (6), pp. 941–946
3 HALL, H.C., and RUSSEK, R.M.: 'Discharge inception and extinction in dielectric voids', *Proc. IEE*, 1954, **101**, pp. 47–58
4 MASON, J.H.: 'The deterioration and breakdown of dielectrics resulting from internal discharges', *Proc. IEE*, 1951, **98**, (1), pp. 44–59
5 CRICHTON, G.C., KARLSSON, P.W., and PEDERSON, A.: 'Partial discharges in ellipsoidal and spheroidal voids', *IEEE Trans. Electr. Insul.*, 1989, **24**, (2), pp. 335–342
6 Bartnikas, R., McMahon, E.J. (Eds.): 'Engineering dielectrics, vol. 1, Corona measurement and interpretations', ASTM, STP669, 1979
7 TANAKA, T.: 'Internal partial discharge and material degradation', *IEEE Trans. Electr. Insul.*, 1986, **21**, (6), pp. 899–905
8 KIND, D., and KONIG, D.: 'AC breakdown of epoxy resins by partial discharges in voids', *IEEE Trans. Electr. Insul.*, 1968, **3**, (2), pp. 40–46
9 KODOLL, W.R., KARNER, H.C., and TANAKA, T.: 'Internal partial discharge resistivity testing', *CIGRE*, 1988, pp. 11504/1–7
10 IEC Publication 270, 'Partial discharge measurements', 1981
11 'Tentative methods of conditioning plastics and electrical insulating materials for testing', D 618-47 T, ASTM
12 'Tentative methods of sampling and testing untreated paper used in electrical insulation', D 202 - 47 T, ASTM